

# Fuzzy physical programming for Space Manoeuvre Vehicles trajectory optimization based on hp-adaptive pseudospectral method

Runqi Chai<sup>a</sup>, Al Savvaris<sup>a</sup>, Antonios Tsourdos<sup>a</sup>

<sup>a</sup>*School of Aerospace, Transport and Manufacturing, Cranfield University, Bedfordshire, MK43 0AL, United Kingdom*

---

## Abstract

In this paper, a fuzzy physical programming (FPP) method has been introduced for solving multi-objective Space Manoeuvre Vehicles (SMV) skip trajectory optimization problem based on hp-adaptive pseudospectral methods. The dynamic model of SMV is elaborated and then, by employing hp-adaptive pseudospectral methods, the problem has been transformed to nonlinear programming (NLP) problem. According to the mission requirements, the solutions were calculated for each single-objective scenario. To get a compromised solution for each target, the fuzzy physical programming (FPP) model is proposed. The preference function is established with considering the fuzzy factor of the system such that a proper compromised trajectory can be acquired. In addition, the NSGA-II is tested to obtain the Pareto-optimal solution set and verify the Pareto optimality of the FPP solution. Simulation results indicate that the proposed method is effective and feasible in terms of dealing with the multi-objective skip trajectory optimization for the SMV.

*Keywords:* Space Manoeuvre Vehicles, fuzzy physical programming, hp-adaptive pseudospectral, nonlinear programming, multi-objective.

---

## 1. Introduction

Over the past couple of decades, trajectory optimization problems in terms of reentry vehicle [1, 2, 3, 4, 5, 6] have attracted significant attention. One of the

---

*Email addresses:* r.chai@cranfield.ac.uk (Runqi Chai), a.savvaris@cranfield.ac.uk (Al Savvaris)

2017年3月23日

current objectives is the development of Space Manoeuvre Vehicles(SMV) for a  
5 dynamic mission profile. The Mach number and the flight altitude of the reentry  
vehicle vary largely during the whole reentry phase, the aerodynamic feature of  
the vehicle has large uncertainties and nonlinearities. Due to these reasons, the  
use of numerical methods to handle these types of problems is commonly used.  
Numerical methods for solving optimal control problems are divided into two  
10 major classes: indirect methods and direct methods[7, 8, 9, 10]. However, it is  
very difficult to solve the trajectory design problem by using indirect methods  
based on maximum principle. Therefore, direct optimization method has been  
widely used for trajectory optimization. Applying direct methods meant the  
development of several discrete methods[11].

15 In recent years, collocation methods for transforming optimal control prob-  
lems have increased in popularity [12, 13]. There are two main kinds of col-  
location methods, local collocation method such as the direct collocation and  
global collocation method e.g. the pseudospectral [14, 15, 16]. In a pseudospec-  
tral method, the collocation points are based on quadrature rules and the basis  
20 function are Lagrange or Chebyshev polynomials. In contrast to the direct col-  
location method, pseudospectral method usually divides the whole time history  
into a single mesh interval whereas its counterpart, direct collocation, divides  
time interval into several equal step subintervals and the convergence is achieved  
by adding the degree of the polynomial. To improve accuracy and computation-  
25 al efficiency using pseudospectral method, L. Darby presented a hp-strategy in  
[17, 18, 19]. By adding collocation points in a certain mesh interval or dividing  
the current mesh into subintervals simultaneously, the accuracy of interpolation  
can be improved dramatically.

Generally, the traditional trajectory design usually aims at one single ob-  
30 jective, for example, minimizing the aerodynamic heating, maximizing the cross  
range, etc. However, in reality, for space vehicle trajectory design, most the  
missions contain more than one requirements and this brings the developmen-  
t of multi-objective optimization(MOO)[20]. There are many multi-objective  
methods which are suitable for these kind of problems. Commonly, the method  
35 based on weighting factors is widely used to transform different criterions into  
only one single objective but it is difficult to determine the weight coefficients.  
In 1996, Messac designed a physical programming(PP) method to convert the  
objectives [21, 22], which removes the information of priority and weight coeffi-

cients. But in practice, usually there are some fuzzy factors in the real system  
 40 and because of this, a fuzzy physical programming method is proposed in this  
 paper.

The mission scenario investigated in this paper focuses on the atmospheric  
 skip hopping, targeting the entry into the atmosphere down to a predetermined  
 position (predetermined altitude given by the industrial sponsor of this project)  
 45 and the required controls involved in returning back to low earth orbit. Studies  
 can be found in the literature regarding the skip reentry of deep-space spacecraft  
 with high speed over first cosmic velocity, however in the scenario considering  
 in this paper, a high thrust engine would be necessary for SMV to return to low  
 earth orbit. The overall mission can be found in Fig.1. General skip reentry can

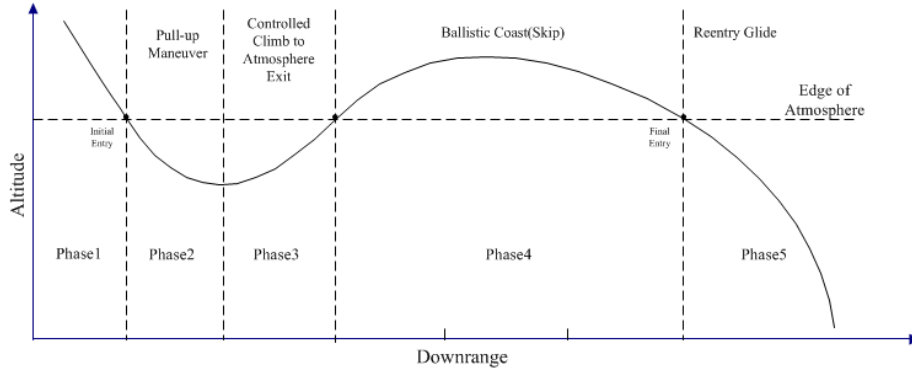


Figure 1: Mission profile

50 be divided into five phases: initial roll, down control, up control, Kepler and  
 final entry. Considering the mission of the SMV is to overfly the ground target  
 with specific altitude, the most challenging phase 2 and 3 will be considered in  
 this paper.

Most of the current studies in trajectory optimization are based on the nu-  
 55 merical simulation. Smirnov et al.[23][24], presented studies in terms of devel-  
 oping mathematical model for evaluation of stochastic numerical errors accumu-  
 lation. Based on the published simulation results, the problem of accumulation  
 of errors cannot be ignored. Therefore, the effect of noise on the trajectory  
 optimization is also considered in this work, and the results are presented in  
 60 Section 5 of this paper.

The paper is organised as follows. In section 2, we introduce the aerodynam-

ic model of the SMV reentry vehicle and some basic principles of the trajectory optimization problem. Section 3 describes the method used to discretize the optimal control problem. Then in section 4 the fuzzy physical programming(FPP) procedures of solving multi-objective SMV trajectory problem is detailed. Following that, section 5 present comparison between solution calculated for each single-objective and the compromised solution generated by employing the FPP approach.

## 2. Problem Description

### 2.1. SMV dynamic model

The Earth is considered as a symmetrical sphere and the earth rotation is ignored. Considering a three degree of freedom dynamic equations of SMV reentry vehicle:

$$\begin{aligned}
\dot{r} &= V \sin \gamma \\
\dot{\theta} &= \frac{V \cos \gamma \sin \psi}{r \cos \phi} \\
\dot{\phi} &= \frac{V \cos \gamma \cos \psi}{r} \\
\dot{V} &= \frac{T \cos \alpha - D}{m} - g \sin \gamma \\
\dot{\gamma} &= \frac{L \cos \sigma + T \sin \alpha}{mV} + \left( \frac{V^2 - gr}{rV} \right) \cos \gamma \\
\dot{\psi} &= \frac{L \sin \sigma}{mV \cos \gamma} + \frac{V}{r} \cos \gamma \sin \psi \tan \phi \\
\dot{m} &= - \frac{T}{I_{sp} g} \\
\dot{\alpha} &= K_{\alpha} (\alpha_c - \alpha) \\
\dot{\sigma} &= K_{\sigma} (\sigma_c - \sigma) \\
\dot{T} &= K_T (T_c - T)
\end{aligned} \tag{1}$$

where  $r$  is the radial distance from the Earth center to the vehicle,  $\theta$  and  $\phi$  are the longitude and latitude,  $V$  is the Earth-relative velocity,  $\gamma$  is the relative flight-path angle,  $\psi$  is the relative velocity heading angle measured clockwise from the north,  $m$  is the mass of the vehicle,  $t$  is time, control variables are angle of attack  $\alpha_C$ , bank angle  $\sigma_C$  and thrust  $T_C$ , respectively. In reality, the real control variables cannot change dramatically (i.e. from lower bound to

80 upper bound). Therefore, in the model provided (1), three rate constraints are introduced by using the technique of first order lag which can be concluded to the last three equations in (1).

The atmosphere model, lift  $L$  and drag  $D$  can be defined as:

$$\begin{aligned} g &= \frac{\mu}{r^2} & \rho &= \rho_0 \exp \frac{r-r_0}{h_s} \\ L &= \frac{1}{2}\rho V^2 C_L S & D &= \frac{1}{2}\rho V^2 C_D S \end{aligned} \quad (2)$$

where  $S = 2690ft^2$  is reference area,  $\mu = 1.4076539 \times 10^{16} ft^3/s^2$  is gravitational parameter of the earth.  $\rho$  is density of atmosphere and  $\rho_0 = 0.002378slug/ft^3$  is density of atmosphere at sea-level.  $r_0 = 20902900ft$  is Earth' s radius,  $C_L$  and  $C_D$  are lift and drag coefficient determined by angle of attack  $\alpha$  and  $Ma$ , respectively,  $g$  is gravity acceleration.

The drag and lift coefficient can be determined by the following equations:

$$\begin{aligned} C_D &= C_{D0} + C_{D1}\alpha + C_{D2}\alpha^2 \\ C_L &= C_{L0} + C_{L1}\alpha \end{aligned} \quad (3)$$

where  $C_{L0} = -0.2070, C_{L1} = 1.676, C_{D0} = 0.07854, C_{D1} = -0.3529, C_{D2} = 2.040$ .

## 2.2. Reentry process constraints

SMV reentry process should satisfy some constraints due to safety reasons and also depending on the mission requirements. These constraints can be summarised as initial and terminal constraints, path constraints and boundary constraints.

### 2.2.1. Initial and terminal constraints

The complete mission can be divided into two phases, the descent phase and exit phase. Due to the mission requirement, the state variables at minimum decent point are specified. The initial conditions of all the states are:

$$[r, \phi, \theta, V, \gamma, \psi, m, \alpha, \sigma, T] = [r_0, \phi_0, \theta_0, V_0, \gamma_0, \psi_0, m_0, \alpha_0, \sigma_0, T_0] \quad (4)$$

On the other hand, at the minimum altitude point and final point(i.e. final point to return back into low earth orbit), hence complete one hop, the terminal altitude constraints are:

$$[r(1), r(f)] = [r_b, r_f] \quad (5)$$

105 where  $r(1)$  and  $r(f)$  stand for altitude value at bottom point and final time, respectively.

### 2.2.2. Path constraints

During the whole time period, to protect the structure of reentry vehicle, in simulation the SMV model need to satisfy strict path constraint, which can  
110 be summarised as follows:

$$\begin{aligned} \dot{Q}_d &= K_Q \rho^{0.5} V^{3.07} (c_0 + c_1 \alpha + c_2 \alpha^2 + c_3 \alpha^3) < Q_{dmax} \\ P_d &= \frac{1}{2} \rho V^2 < P_{dmax} \\ n_L &= \frac{\sqrt{L^2 + D^2}}{mg} < n_{Lmax} \end{aligned} \quad (6)$$

where  $c_0 = 1.067$ ,  $c_1 = -1.101$ ,  $c_2 = 0.6988$ ,  $c_3 = -0.1903$  and  $K_Q = 9.289 \times 10^{-9} \text{ Btu} \cdot \text{s}^{2.07} / \text{ft}^{3.57} / \text{slug}^{0.5}$ .  $Q_{dmax}$ ,  $P_{dmax}$  and  $n_{Lmax}$  represents allowable maximum heating rate, dynamic pressure and acceleration, respectively.

### 2.2.3. Boundary constraints

115 For the SMV, the states should be limited as:

$$\begin{aligned} r_{min} &\leq r \leq r_{max} & \theta_{min} &\leq \theta \leq \theta_{max} \\ \phi_{min} &\leq \phi \leq \phi_{max} & V_{min} &\leq V \leq V_{max} \\ \gamma_{min} &\leq \gamma \leq \gamma_{max} & \psi_{min} &\leq \psi \leq \psi_{max} \\ m_{min} &\leq m \leq m_{max} & \alpha_{min} &\leq \alpha \leq \alpha_{max} \\ \sigma_{min} &\leq \sigma \leq \sigma_{max} & T_{min} &\leq T \leq T_{max} \end{aligned} \quad (7)$$

and the boundaries in terms of the control variables are defined as:

$$\begin{aligned} \alpha_{c(min)} &\leq \alpha_c \leq \alpha_{c(max)} \\ \sigma_{c(min)} &\leq \sigma_c \leq \sigma_{c(max)} \\ T_{c(min)} &\leq T_c \leq T_{c(max)} \end{aligned} \quad (8)$$

## 2.3. Objective function

To ensure the SMV has enough fuel carry-out several skip loops and maximise the number of hops, the first objective would be to minimize the fuel consumption, i.e., maximize final mass value, during the whole process. Moreover,  
120 the total aerodynamic heating is very important and it can have a serious implications on the SMV integrity structure. In addition, it is not desirable to have too many oscillations during the mission as it will also impact the integrity of the structure. On the other hand, a high final velocity will provide more

125 kinetic energy for the vehicle and hence reduce the overall mission time which is desirable. Therefore, the objective functions are selected in the analysis.

1). Maximizing the final mass:

$$\max J_1 = m(t_f) \quad (9)$$

2). Minimizing the total aerodynamic heating:

$$\min J_2 = \int_{t_0}^{t_f} Q(t) dt \quad (10)$$

3). Minimizing the oscillation:

$$\min J_3 = \int_{t_0}^{t_f} \gamma(t)^2 dt \quad (11)$$

130 4). Maximizing the final velocity:

$$\max J_4 = V(t_f) \quad (12)$$

5). Minimizing the final time:

$$\min J_5 = t_f \quad (13)$$

By setting the cost function described in Eq.(9)-Eq.(13), the SMV trajectory problem can be considered as an optimal control problem which has minimum or maximum cost function value and satisfy the initial and terminal state constraints, control variable constraints, three path constraints and dynamic equations.  
135

### 3. Global collocation method

To solve the problem using the numerical method, the trajectory design problem needs to be transformed to nonlinear programming(NLP) and the basic method used in this paper is the pseudospectral method. Compared to local direct collocation, it uses the initial time point  $t_0$  and terminal time point  $t_f$  as two node points and removes numbers of small time segment introduced in direct collocation method. In other words, by using pseudospectral method, there is only one time interval  $[t_0, t_f]$  and can use orthogonal polynomial to approximate the state and control for the whole time history.  
145

Assuming the time interval of an optimal control problem is  $[t_0, t_f]$ , the pseudospectral method must be used on the  $[-1, 1]$  and therefore, we transform the time interval by using:

$$t = \frac{t_f - t_0}{2}\tau + \frac{t_f + t_0}{2} \quad (14)$$

Following the transformation of the time interval to the values  $[-1, 1]$ , the next step is to generate the approximation of state and control. In the Pseudospectral method, the state and control of an optimal control problem are approximated as:

$$\begin{aligned} x(\tau) &\approx X(\tau) = \sum_0^N X_i L_i(\tau) \\ u(\tau) &\approx U(\tau) = \sum_0^N U_i L_i(\tau) \end{aligned} \quad (15)$$

where  $\tau \in [-1, 1], L_i(\tau), (i = 0, \dots, N)$  are the collocation points and a basis of Lagrange polynomials, respectively. The LGR points are used as the collocation point. LGR points are the root of linear combination of Legendre polynomials which can be written as:

$$P_{K-1}(\tau) + P_K(\tau) = 0 \quad (16)$$

where the  $K$ th order Legendre polynomial  $P_K(\tau)$  is

$$P_K(\tau) = \frac{1}{2^K K!} \frac{d^K}{d\tau^K} [(\tau^2 - 1)^K] \quad (17)$$

In order to improve the performance of global pseudospectral method, hp-strategy has been developed for mesh refinement. The goal of the hp-adaptive algorithm is to improve the accuracy of the solution in an effective manner by judging if a certain mesh interval has met a specified tolerance. If the mesh cannot meet the accuracy tolerance, then the number of nodes or intervals should be changed either by increasing the degree of the polynomial in the mesh interval or dividing the mesh into several segments.

Let  $e_{max}$  mean the maximum error at  $i$ th collocation point. If  $e_{max}$  can satisfy the tolerance, then can stop the iteration since collocation points in the  $k$ th interval can reach the tolerance. Otherwise, it should be divided into subintervals or more collocation points are added.



Whether we need to divide the interval into segments or add collocation  
170 points, this can be determined by using curvature. If the value of curvature  
overpass the tolerance, then the trajectory in the current interval is very noisy  
and it should be divided into new subintervals. On the other hand, if the  
tolerance can be satisfied, meaning the trajectory is flat in current interval and  
the accuracy can be improved by adding more collocation points.

175 By using the approach described above, the dynamic model can be trans-  
formed to algebraic constraints. Combining with the constraints mentioned in  
section 2.2 and cost function presented in section 2.3, the SMV trajectory prob-  
lem is converted to a nonlinear programming problem(NLP) with state and  
control variables at collocation points.

#### 180 4. Fuzzy physical programming

The multi-objective optimization problem of SMV trajectory design can  
be solved using the Fuzzy Physical Programming(FPP) method. FPP involves  
converting a multi-objective problem into a single objective problem using fuzzy  
performance functions that capture the decision maker's preferences, and after  
185 that solving this transformed single-objective optimization to find a compromise  
solution.

##### *4.1. Physical programming*

To generate a preferred compromise during multi-objective system opti-  
mization, a method called physical programming(PP) is introduced. The way  
190 that PP captures the designer's preferences is by using preference function-  
s. Compared with other multi-objective methods, the application of PP does  
not require the decision maker to specify weights for different object functions.  
Rather, the decision maker needs to define ranges of differing degrees of desir-  
ability for each objective function. It has been shown that PP offers the user  
195 several advantages, for example, it can reduce computational effort and time,  
and at the same time, eliminate iterative selection of weights and priorities of  
objective functions.

The objective functions are classified into four types:

- (i) Class 1-S: smaller-is-better(minimization).
- 200 (ii) Class 2-S: larger-is-better(maximization).

- (iii) Class 3-S: value-is-better(seek value).
- (iv) Class 4-S: range-is-better(seek range).

Take class 1-S as an example, the boundary of the preference region is represented by some values of objective function and there are six ranges for classes 1-S and 2-S defined as follows:

- (i) Ideal range ( $f_i \leq f_{i1}$ )
- (ii) Desirable range ( $f_{i1} \leq f_i \leq f_{i2}$ )
- (iii) Tolerable range ( $f_{i2} \leq f_i \leq f_{i3}$ )
- (iv) Undesirable range ( $f_{i3} \leq f_i \leq f_{i4}$ )
- (v) Highly undesirable range ( $f_{i4} \leq f_i \leq f_{i5}$ )
- (vi) Unacceptable range ( $f_i \geq f_{i5}$ )

The parameters  $f_{i1} - f_{i5}$  are physically meaningful values that are specified by the decision maker to quantify the preference functions with respect to the  $i$ th cost function. In the paper, these parameters are computed by single objective optimization and the values can be determined using the following payoff table constructed by optimal solution of single objective optimization(see Table 1).

Table 1: Payoff table

	$f_1$	$f_2$	$f_3$	$\cdots$	$f_m$
Opt $f_1(x, u)$	$f_1(x_1^*, u_1^*)$	$f_2(x_1^*, u_1^*)$	$f_3(x_1^*, u_1^*)$	$\cdots$	$f_m(x_1^*, u_1^*)$
Opt $f_2(x, u)$	$f_1(x_2^*, u_2^*)$	$f_2(x_2^*, u_2^*)$	$f_3(x_2^*, u_2^*)$	$\cdots$	$f_m(x_2^*, u_2^*)$
Opt $f_3(x, u)$	$f_1(x_3^*, u_3^*)$	$f_2(x_3^*, u_3^*)$	$f_3(x_3^*, u_3^*)$	$\cdots$	$f_m(x_3^*, u_3^*)$
$\vdots$	$\vdots$	$\vdots$	$\vdots$	$\vdots$	$\vdots$
Opt $f_m(x, u)$	$f_1(x_m^*, u_m^*)$	$f_2(x_m^*, u_m^*)$	$f_3(x_m^*, u_m^*)$	$\cdots$	$f_m(x_m^*, u_m^*)$

For instance,  $(x_j^*, u_j^*)$  is the optimal solution of the  $j - th$  single objective optimization, then  $f_{i1}$  can be achieved by:

$$f_{i1} = \min_{j=1, \dots, m} f_i(x_j^*, u_j^*), \quad i = 1, \dots, m. \quad (18)$$

Once the range parameters have been determined for each objective function, preference functions are constructed. Considering the case of class 1-S, the preference function  $p_i(f_i(X))$  are defined as follows, and the preference function for class 2-S is the mirror image of class 1-S.

$$p_i^k = A_0(\xi_i^k)p_{i(k-1)} + A_1(\xi_i^k)p_{ik} + \overline{A_0}(\xi_i^k, \lambda_i^k)s_{i(k-1)} + \overline{A_1}(\xi_i^k, \lambda_i^k)s_{ik} \quad (19)$$

where  $\xi_i^k = (f_i - f_{i(k-1)})/(f_{ik} - f_{i(k-1)})$  and  $0 < \xi_i^k < 1$ ,  $\lambda_i^k = (f_{ik} - f_{i(k-1)})$ ,  $k$  is the number of region and  $k = 2, 3, 4, 5$ . As can be seen from Eq.(19), for each  
 225 region, the preference function takes the form of a spline segment which can be defined by its value and slope.

$$s_{ik} = \frac{\partial p_i^k}{\partial f_i^k} \Big|_{f_i^k = f_{ik}} \quad (20)$$

$$A_0(\xi) = \frac{1}{2}\xi^4 - \frac{1}{2}(\xi - 1)^4 - 2\xi + \frac{3}{2} \quad (21)$$

$$A_1(\xi) = -\frac{1}{2}\xi^4 - \frac{1}{2}(\xi - 1)^4 + 2\xi - \frac{1}{2} \quad (22)$$

$$\overline{A_0}(\xi, \lambda) = \lambda \left[ \frac{1}{8}\xi^4 - \frac{3}{8}(\xi - 1)^4 - \frac{1}{2}\xi + \frac{3}{8} \right] \quad (23)$$

230

$$\overline{A_1}(\xi, \lambda) = \lambda \left[ \frac{3}{8}\xi^4 - \frac{1}{8}(\xi - 1)^4 - \frac{1}{2}\xi + \frac{1}{8} \right] \quad (24)$$

In the end, for the first region, the preference function can be defined by an exponential function:

$$p_i^1 = p_{i1} \exp\left[\left(\frac{s_i^1}{p_{i1}}\right)(f_i - f_{i1})\right] \quad (25)$$

#### 4.2. Fuzzy preference

To take into account the decision maker's physical understanding of the de-  
 235 sired design outcomes, a fuzzy preference is introduced during the optimization process. In this way, it can enable the decision maker to control the optimization to some extent. Suppose that the preference function of the  $i - th$  objectives belongs to Class-1, we define the parameter  $f_{ik}$  as a normal fuzzy number  $\tilde{f}_{ik}$  and therefore, its membership function follows the form:

$$\mu_{\tilde{f}_{ik}}(f_i) = \exp^{-\left[\frac{f_i - f_{ik}}{\delta_{ik}}\right]^2}, \quad \delta_{ik} > 0 \quad (26)$$

240 where  $\delta_{ik}$  is the fuzzy parameter of the  $k - th$  boundary of preference function and it can be defined based on [25, 26]. Then the fuzzy preference function can be summarised as follows:

$$f_{p_{ik}}(\tilde{f}_{ik}) = \frac{\int_{f_i(X) - 3\delta_{ik}}^{f_i(X) + 3\delta_{ik}} \bar{f}_i(f_i) \mu_{\tilde{f}_{ik}}(f_i) df_i}{\int_{f_i(X) - 3\delta_{ik}}^{f_i(X) + 3\delta_{ik}} \mu_{\tilde{f}_{ik}}(f_i) df_i} \quad (27)$$

$\bar{f}_i(f_i)$  is the preference function of  $i$ -th objective function without considering fuzzy factor.

245 **4.3. Fuzzy programming problem**

By defining the fuzzy preference function and range parameters for each objective function, the compromise solution can be achieved by solving the optimization problem as follows:

$$\left\{ \begin{array}{ll} \min P = \log_{10} \left\{ \frac{1}{n_s} \sum_{i=1}^{n_s} f_{p_{ik}}(\tilde{f}_{ik}) \right\}, & \\ f_i(X) \leq f_{i5}, & \text{for class 1-S;} \\ f_i(X) \geq f_{i5}, & \text{for class 2-S;} \\ f_{i5L} \leq f_i(X) \leq f_{i5R}, & \text{for class 3-S;} \\ f_{i5L} \leq f_i(X) \leq f_{i5R}, & \text{for class 4-S.} \end{array} \right. \quad (28)$$

where  $n_s$  is the number of ranges associated with the problem and the range limits can be specified by defining the pay-off table. Take the case of Class 1-S  
250 as an example, the fuzzy preference function is shown in Fig.2.

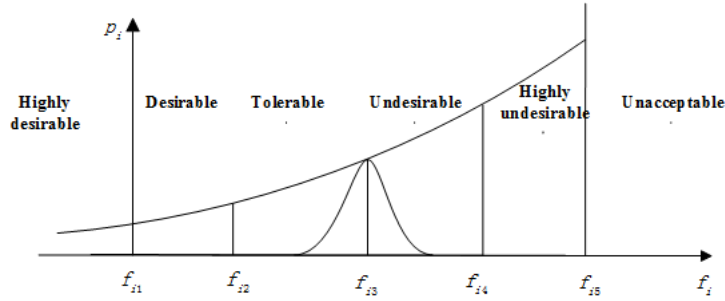


Figure 2: Fuzzy preference function for Class 1-S

**5. Simulation results**

**5.1. Parameters setting**

The maximum values of heat flux, dynamic pressure and load factor are  
255  $Q_{dmax} = 200 \text{ Btu/ft}^2/\text{s}$ ;  $P_{dmax} = 13406.4583 \text{ Pa}$ ;  $n_{Lmax} = 2.5$ , respectively. The initial and terminal conditions of the entire process and boundary constraints can be found in Table 2.

Table 2: Parameters setting

	Initial	Bottom	Terminal	Minimum	Maximum
$r(\text{ft})$	21162900	21066900	21162900	21066900	21162900
$\theta(\text{deg})$	0	free	free	-180	180
$\phi(\text{deg})$	0	free	free	-70	70
$V(\text{ft/s})$	25600	free	free	2000	45000
$\gamma(\text{deg})$	-1	free	free	-80	80
$\psi(\text{deg})$	90	free	free	-180	180
$m(\text{sl})$	6309.4	free	free	1370.4	6309.4
$\alpha(\text{deg})$	17.43	free	free	0	40
$\sigma(\text{deg})$	-75	free	free	-90	1
$T(N)$	0	free	free	0	2000000

The specific boundary conditions are given by the industrial sponsor Lockheed Martin Space Systems Company and only the first hop is taken into account in the paper. The initial altitude is around  $80\text{km}$  where is the edge of atmosphere.

### 5.2. Time history of the state and control

Firstly, the optimization results for each single objective function according to the dynamic model, objectives and constraints given in Section 2 are generated. The results are shown in Figs.3-7.

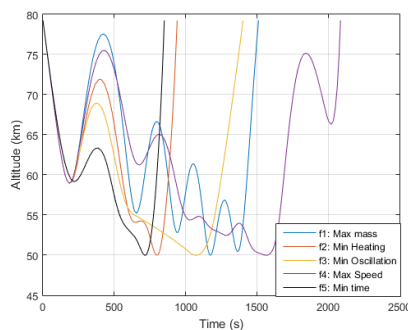


Figure 3: Altitude for different objective function

As can be seen from Fig.3-7, conflicts exist between each objective function, therefore it is impossible to find a solution optimizing each cost function. For

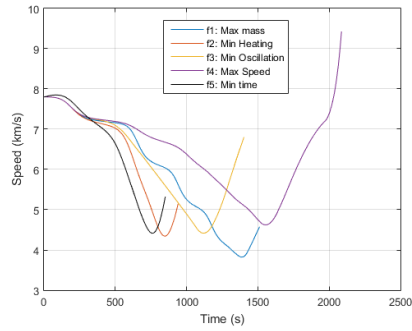


Figure 4: Speed for different objective function

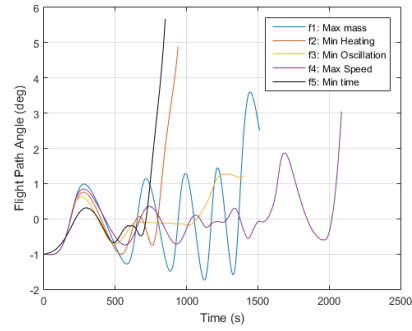


Figure 5: Flight path angle for different objective function

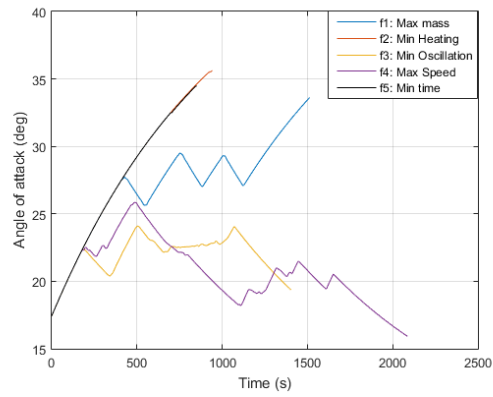


Figure 6: Angle of attack for different objective function

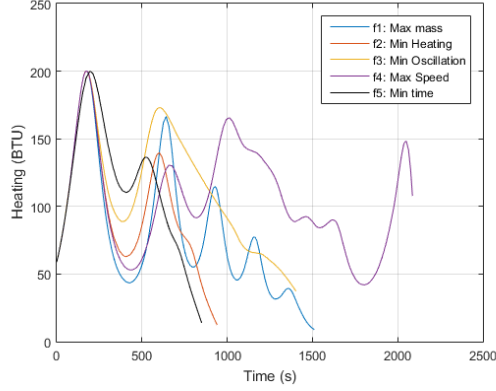


Figure 7: Aerodynamic heating for different objective function

example, in the case of maximizing final velocity, if there is no compromised  
 270 procedure, then to achieve a higher speeds, the SMV is tending to complete  
 the mission with longer time and accelerating during the whole time period,  
 which means it is trying to consume all the fuel. Hence, after reaching the low  
 earth orbit, the SMV has no fuel left to continue the mission. Similar with [27]  
 presented by Hu and Xin, to see the results more clearly, the payoff table results  
 are tabulated in Table.3.

Table 3: Payoff table

	$J_1$	$J_2$	$J_3$	$J_4$	$J_5$
max $J_1$	4437.5	121.86	$8.840 \times 10^{-3}$	15013.5	1512.04
min $J_2$	3971.2	75.38	$2.459 \times 10^{-2}$	16887.4	940.96
min $J_3$	1667.7	195.12	$7.443 \times 10^{-6}$	22327.3	1403.22
max $J_4$	1370.4	217.63	$9.376 \times 10^{-3}$	30937.6	2086.42
min $J_5$	2782.1	89.17	$7.642 \times 10^{-5}$	17467.5	850.56

275 From the pay-off table, we can conclude the boundary based on the best  
 solution and worst solution from single objectives results that:  $f_{11} = 4427.5$ ,  
 $f_{21} = 75.38$ ,  $f_{31} = 7.443 \times 10^{-6}$ ,  $f_{41} = 30937.6$ ,  $f_{51} = 850.56$  and  $f_{15} = 1370.4$ ,  
 $f_{25} = 217.63$ ,  $f_{35} = 2.459 \times 10^{-2}$ ,  $f_{45} = 15013.5$ ,  $f_{55} = 2086.42$ . Then the FFP

model can be obtained as follows:

$$\left\{ \begin{array}{l}
 \min \quad \log_{10}\{\frac{1}{5} \sum_{i=1}^5 f_{p_{ik}}(\tilde{f}_{ik})\}, \\
 f_1(X) \geq 1370.4 \\
 f_2(X) \leq 217.63 \\
 f_3 \leq 2.459 \times 10^{-2} \\
 f_4 \geq 15013.5 \\
 f_5 \leq 2086.42 \\
 \dot{Q}_d = K_Q \rho^{0.5} V^{3.07} (c_0 + c_1 \alpha + c_2 \alpha^2 + c_3 \alpha^3) < 200 BTU/ft^2/s \\
 P_d = \frac{1}{2} \rho V^2 < 13406.4583 Pa \\
 n_L = \frac{\sqrt{L^2 + D^2}}{mg} < 2.5 \\
 (4), (5), (7) \text{ and } (8)
 \end{array} \right. \quad (29)$$

280 where the first equation of the optimization objective of (29) is to optimize  
all the objectives by minimizing the preference function values. By solving  
the model illustrated above, we can achieve the compromised time history of  
each state and control. The corresponding trajectories generated by using PP  
and FPP for optimization parameters and constraint can be found in Figs.8-16,  
285 respectively.

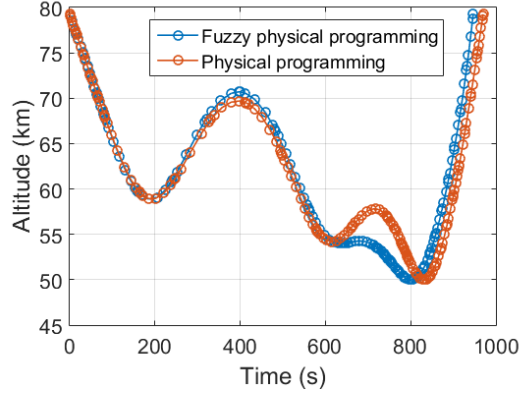


Figure 8: Altitude for FPP and PP

To further compare the results generated from PP and FPP, simulation re-  
sults were done in order to verify the Pareto optimality of PP and FPP solution  
by comprising with the Pareto-optimal solutions obtained using NSGA-II and  
the weighted method, which can be seen in Table 5. NSGA-II shares a simi-



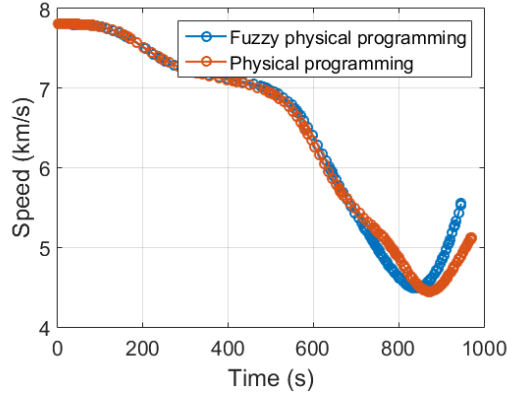


Figure 9: Speed for FPP and PP

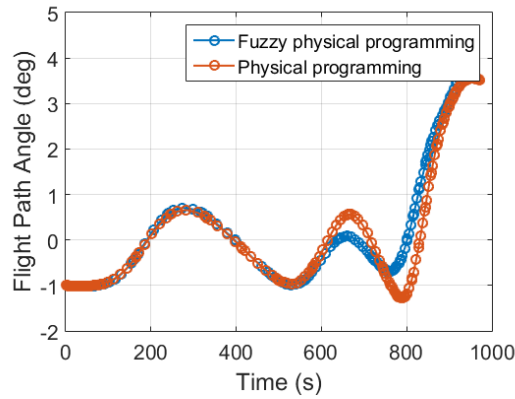


Figure 10: Flight path angle for FPP and PP

lar idea with PP of transforming the multi-objectives to a well-designed single  
 290 fitness function and creates a number of fronts. During the optimization pro-  
 cedure, the first front is generated as the set of solutions that has the highest  
 fitness value and is not dominated by any other solutions in the current popu-  
 lation. For the NSGA-II simulation, the population size is 200, the maximum  
 295 number of generations is 500 while the tournament selection scale is 3. The  
 probability of crossover and mutation are 0.8 and 0.1, respectively.

The Pareto fronts, generated by NSGA-II, PP, FPP and weighted method(i.e.  
 solutions can be found in Table.4), are projected onto two plane shown in Fig.17  
 and Fig.18. From the plane of minimizing terminal time versus minimizing to-

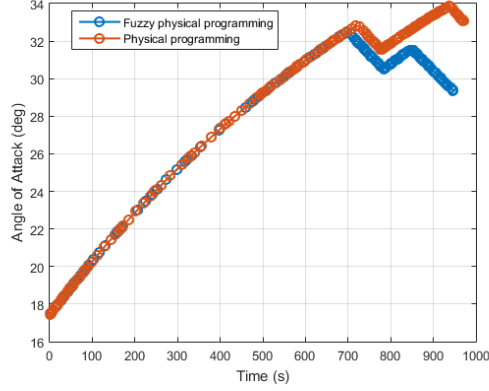


Figure 11: Angle of attack FPP and PP

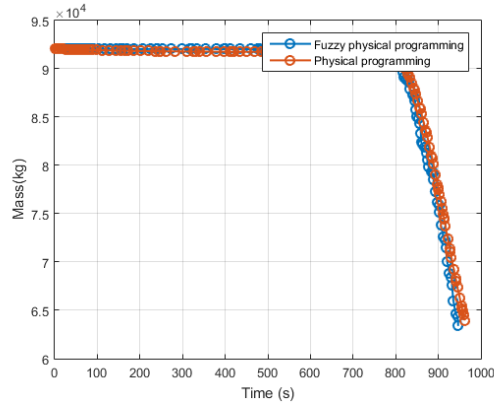


Figure 12: Mass for FPP and PP

Table 4: Optimization results for weighted method

Weights	Objective values( $J_1, J_2, J_3, J_4, J_5$ )
(0.30, 0.10, 0.10, 0.30, 0.20)	(4330.2, 97.57, $7.93 \times 10^{-4}$ , 16770.7, 963.9)
(0.35, 0.15, 0.15, 0.20, 0.15)	(4342.3, 99.48, $7.63 \times 10^{-4}$ , 16502.2, 975.5)
(0.40, 0.20, 0.20, 0.10, 0.10)	(4378.7, 105.42, $6.75 \times 10^{-4}$ , 16492.2, 988.1)

300 tal heating and maximizing final velocity versus maximizing final mass, it is clear that both PP and FPP can get the solutions around the Pareto frontier generated by NSGA-II while it is hard for weighted method to generate a Pareto-optimal solution. Specifically, the compromised solution obtained by

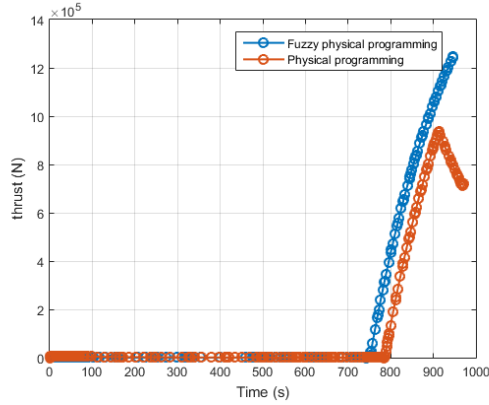


Figure 13: Thrust for FPP and PP

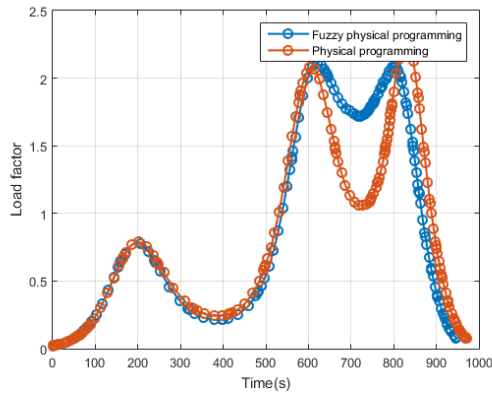


Figure 14: Load factor for different objective function

FPP can have a better preference than its counterpart PP, hence it has smaller  
 305 variance with the Pareto frontier. As FPP approach is designed to generate  
 a single Pareto-optimal solution in one run whereas NSGA-II approach is de-  
 signed to obtain hundreds of solutions in one run, therefore, FPP is definitely  
 competitive in computational effort and is more convenient in the numerical  
 experiments and practical use.

310 Table.5 contains the compromised solution for each objective function and  
 the variance proportion. As can be seen from Table.5, the maximum variance  
 percentage can reach around 8.4% , that means if we do not consider the fuzzy  
 factor, there will be some differences between the calculated solution with com-

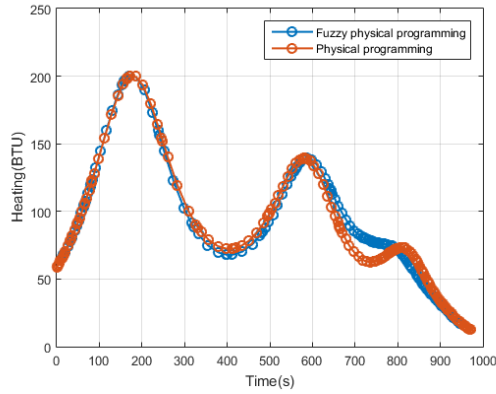


Figure 15: Aerodynamic heating for different objective function

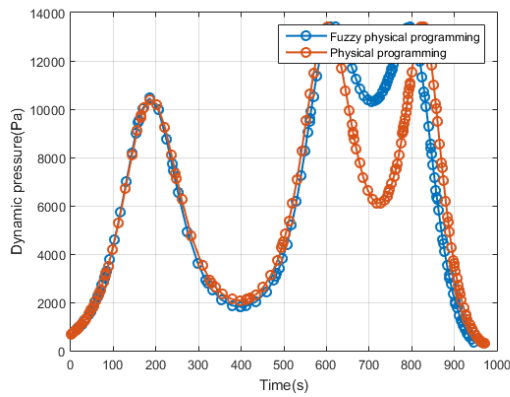


Figure 16: Dynamic pressure for different objective function

pared to the practical solution. Both solutions calculated from PP and FPP  
 315 satisfy the path constraints and for the solution of FPP, it is found that all of  
 the compromised objective values can be successfully obtained. Specifically, the  
 value of  $J_1$  is in the tolerable region whereas the value of  $J_2$  is in the desirable  
 region.  $J_3$  and  $J_5$  are in the tolerable region while the value of  $J_4$  can reach desirable  
 region. This further proves that the combination of hp-adaptive discrete  
 320 method with FPP can be applied to multi-objective optimization for trajectory  
 design problems.

Using the technique of hp-adaptive pseudospectral method, the time history  
 for the states and controls can be much smoother. This can be seen from

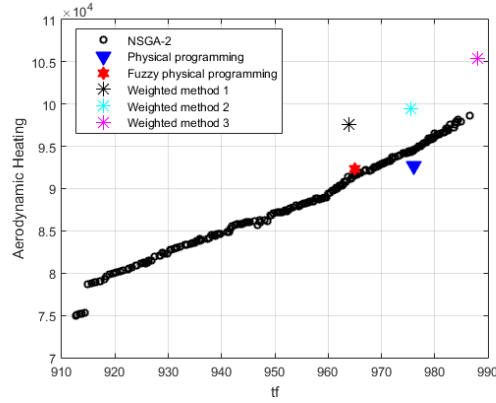


Figure 17: Total heating versus terminal time

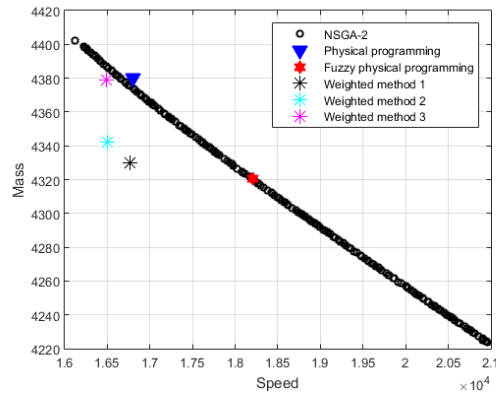


Figure 18: Final mass versus final speed

Table 5: Objective values

	$J_1$	$J_2$	$J_3$	$J_4$	$J_5$
PP	4380.3	92.63	$5.43 \times 10^{-4}$	16798.5	976.06
FPP	4330.1	92.35	$5.01 \times 10^{-4}$	18208.1	965.62
Variance(%)	1.6	0.3	5.9	8.4	1.1

325 Figs.8-16, where the distribution of collocation points tend to be denser at those areas having a high value of curvature, on the other hand, the distribution of collocation points tend to be sparser at those flat areas. That way can control the number of optimization parameters and control the size of NLP problem

effectively. Also, since the trajectory becomes smoother, it is more possible and reasonable for practical use.

330 The accumulation of errors generated from numerical simulation model should be evaluated depending on technique used. The parameters used in model have errors and are modeled in the simulation as a Gaussian white noises. Comparative simulation results are shown in Fig.19-20. It is shown that computational errors accumulation affects the shape of trajectory slightly. The reliability of results can be guaranteed since the hp-strategy used for mesh refinement can improve the accuracy of current mesh grids.

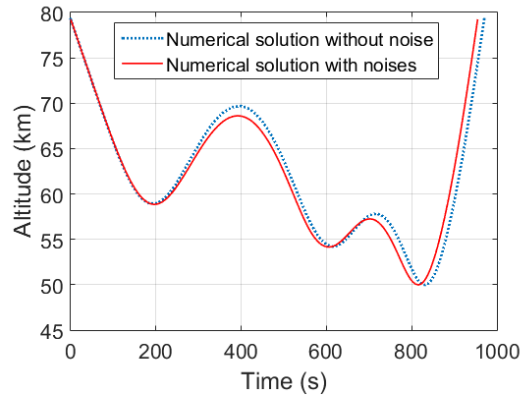


Figure 19: Altitude vs time

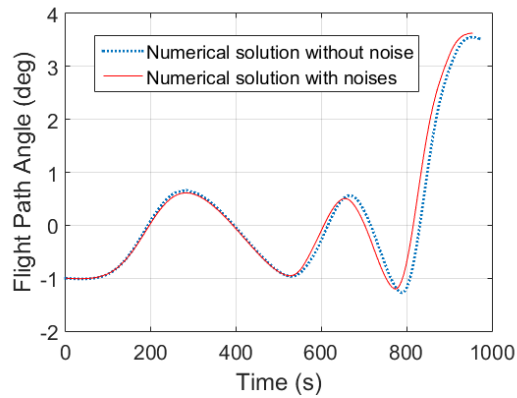


Figure 20: Flight path angle vs time

In summary, all the figures and data provided earlier confirm the feasibility

of the proposed combination method in terms of SMV trajectory design problem.

## 6. Conclusions

340 In order to design a proper trajectory for the SMV, the previously proposed  
single-objective optimization formulation were extended to multi-objective op-  
timization, including maximum final mass, minimum total aerodynamic heat-  
ing, minimum oscillation, maximum final velocity and minimum final time. A  
multi-objective optimization method FPP based on hp-adaptive pseudospectral  
345 method was proposed. When considering the fuzzy factor for the system, in  
FPP, fuzzy preference function is introduced to adjust the boundary defined by  
the decision maker. The simulation results show that there are significant dif-  
ferences between each single-objective solution and by using the FPP method,  
a compromised solution can be obtained. A comparison was made between the  
350 results obtained by using FPP and NSGA-II, which showed that the method  
proposed in this paper can have a better preference in terms of generating Pare-  
to optimal solution than other methods and therefore, it tends to be feasible for  
the SMV trajectory design problem and the definition of the fuzzy function is  
important.

## 355 References

- [1] C. Gan, W. Zi-ming, X. Min, C. Si-lu, Genetic Algorithm Optimization of R-  
LV Reentry Trajectory, International Space Planes and Hypersonic Systems  
and Technologies Conferences, American Institute of Aeronautics and As-  
tronautics, doi:10.2514/6.2005-3269. doi:doi:10.2514/6.2005-326910.  
360 2514/6.2005-3269.
- [2] Z. Kenan, C. Wanchun, Reentry Vehicle Constrained Trajectory Opti-  
mization, International Space Planes and Hypersonic Systems and Tech-  
nologies Conferences, American Institute of Aeronautics and Astronau-  
tics, doi:10.2514/6.2011-2231. doi:doi:10.2514/6.2011-223110.2514/  
365 6.2011-2231.
- [3] A. Rajesh, Reentry Trajectory Optimization: Evolutionary Approach,  
Multidisciplinary Analysis Optimization Conferences, American Institute  
of Aeronautics and Astronautics, doi:10.2514/6.2002-5466. doi:doi:10.  
2514/6.2002-546610.2514/6.2002-5466.

- 370 [4] W. Robert, A. Mark, B. Jeffrey, W. Robert, A. Mark, B. Jeffrey, Minimum heating reentry trajectories for advanced hypersonic launch vehicles, Guidance, Navigation, and Control and Co-located Conferences, American Institute of Aeronautics and Astronautics, doi:10.2514/6.1997-3535. doi:doi:10.2514/6.1997-353510.2514/6.1997-3535.
- 375 [5] T. Lips, B. Fritsche, A comparison of commonly used re-entry analysis tools, Acta Astronautica 57 (2) (2005) 312–323.
- [6] M. Reyhanoglu, J. Alvarado, Estimation of debris dispersion due to a space vehicle breakup during reentry, Acta Astronautica 86 (3) (2013) 211–218.
- [7] J. T. Betts, Survey of numerical methods for trajectory optimization, Journal of Guidance, Control, and Dynamics 21 (2) 193–207. doi:10.2514/2.4231.
- 380 [8] I. Mikhail, V. Pavel, K. Alexandr, Numerical Investigation of the EXPERT Reentry Vehicle Aerothermodynamics Along the Descent Trajectory, Fluid Dynamics and Co-located Conferences, American Institute of Aeronautics and Astronautics, doi:10.2514/6.2007-4145. doi:doi:10.2514/6.2007-414510.2514/6.2007-4145.
- 385 [9] G. Peter, W. Klaus, Trajectory optimization using a combination of direct multiple shooting and collocation, Guidance, Navigation, and Control and Co-located Conferences, American Institute of Aeronautics and Astronautics, doi:10.2514/6.2001-4047. doi:doi:10.2514/6.2001-404710.2514/6.2001-4047.
- 390 [10] G. W. Reddien, Collocation at gauss points as a discretization in optimal control, SIAM Journal on Control and Optimization 17 (2) 298–306. doi:doi:10.1137/0317023.
- 395 [11] F. Fariba, I. Ross, Costate estimation by a Legendre pseudospectral method, Guidance, Navigation, and Control and Co-located Conferences, American Institute of Aeronautics and Astronautics, doi:10.2514/6.1998-4222. doi:doi:10.2514/6.1998-422210.2514/6.1998-4222.
- 400 [12] S. Jain, P. Tsiotras, Trajectory optimization using multiresolution techniques, Journal of Guidance, Control, and Dynamics 31 (5) 1424–1436. doi:10.2514/1.32220.



- [13] R. Jeremy, Launch Vehicle Trajectory Optimization Using a Legendre Pseudospectral Method, Guidance, Navigation, and Control and Co-located Conferences, American Institute of Aeronautics and Astronautics, doi:10.2514/6.2003-5640. doi:doi:10.2514/6.2003-564010.2514/6.2003-5640.
- 405
- [14] D. A. Benson, G. T. Huntington, T. P. Thorvaldsen, A. V. Rao, Direct trajectory optimization and costate estimation via an orthogonal collocation method, Journal of Guidance, Control, and Dynamics 29 (6) 1435–1440. doi:10.2514/1.20478.
- 410
- [15] D. W. Bruno, Generation of pseudospectral differentiation matrices i, SIAM Journal on Numerical Analysis 34 (4) 1640–1657. doi:doi:10.1137/S0036142993295545.
- [16] J. Timothy, S. Christopher, F. Franklin, R. Anil, Constrained Trajectory Optimization Using Pseudospectral Methods, Guidance, Navigation, and Control and Co-located Conferences, American Institute of Aeronautics and Astronautics, doi:10.2514/6.2008-6218. doi:doi:10.2514/6.2008-621810.2514/6.2008-6218.
- 415
- [17] D. Christopher, H. William, R. Anil, An Improved Adaptive hp Algorithm using Pseudospectral Methods for Optimal Control, Guidance, Navigation, and Control and Co-located Conferences, American Institute of Aeronautics and Astronautics, doi:10.2514/6.2010-8272. doi:doi:10.2514/6.2010-827210.2514/6.2010-8272.
- 420
- [18] C. L. Darby, W. W. Hager, A. V. Rao, Direct trajectory optimization using a variable low-order adaptive pseudospectral method, Journal of Spacecraft and Rockets 48 (3) 433–445. doi:10.2514/1.52136.
- 425
- [19] G. Divya, H. William, R. Anil, Gauss Pseudospectral Method for Solving Infinite-Horizon Optimal Control Problems, Guidance, Navigation, and Control and Co-located Conferences, American Institute of Aeronautics and Astronautics, doi:10.2514/6.2010-7890. doi:doi:10.2514/6.2010-789010.2514/6.2010-7890.
- 430
- [20] C.-H. Huang, J. Galuski, C. L. Bloebaum, Multi-objective pareto concur-

rent subspace optimization for multidisciplinary design, *AIAA Journal* 45 (8) 1894–1906. doi:10.2514/1.19972.

- 435 [21] K.-P. Lin, Y.-Z. Luo, G.-J. Tang, Multi-objective optimization of space station logistics strategies using physical programming, *Engineering Optimization* 47 (8) 1140–1155. doi:10.1080/0305215X.2014.954568.
- [22] A. Messac, Physical programming - effective optimization for computational design, *AIAA Journal* 34 (1) 149–158. doi:10.2514/3.13035.
- 440 [23] N. N. Smirnov, V. B. Betelin, V. F. Nikitin, L. I. Stamov, D. I. Altoukhov, Accumulation of errors in numerical simulations of chemically reacting gas dynamics, *Acta Astronautica* 117 338–355. doi:http://dx.doi.org/10.1016/j.actaastro.2015.08.013.
- [24] N. N. Smirnov, V. B. Betelin, V. F. Nikitin, Y. G. Phylippov, J. Koo, Detonation engine fed by acetylene-oxygen mixture, *Acta Astronautica* 104 (1) 134–146. doi:http://dx.doi.org/10.1016/j.actaastro.2014.07.019.
- 445 [25] R. V. Tappeta, J. E. Renaud, A. Messac, G. J. Sundararaj, Interactive physical programming: Tradeoff analysis and decision making in multicriteria optimization, *AIAA Journal* 38 (5) 917–926. doi:10.2514/2.1048.
- [26] X. Zhang, H.-Z. Huang, L. Yu, Fuzzy preference based interactive fuzzy physical programming and its application in multi-objective optimization, *Journal of mechanical science and technology* 20 (6) (2006) 731–737.
- 455 [27] C.-F. Hu, Y. Xin, Reentry trajectory optimization for hypersonic vehicles using fuzzy satisfactory goal programming method, *International Journal of Automation and Computing* 12 (2) (2015) 171–181.